Draft 22 April 2020

Cycle 5 NRAO ALMA Development Study Report Technology Development of Quantum-Limited, Ultra-Wideband RF Amplifiers for ALMA: A 65-150 GHz Test Case

O. Noroozian (NRAO)

ABSTRACT

The ALMA 2030 roadmap recommends the development of receivers with larger bandwidth and better sensitivity for improving observation speed. In this 1-year study, we describe progress on the development of a breakthrough amplifier technology called the Traveling-Wave Kinetic Inductance Parametric (TKIP) amplifier that was invented by our collaborators at Caltech/JPL. These paramps are a new type of cryogenic power amplifier applicable in the microwave to THz range (0.001 to 1 THz) that exhibit ultralow noise reaching the fundamental quantum limits set by Heisenbergs uncertainty principle, along with very wide instantaneous bandwidth (an octave or more). The study of these amplifiers is considered strategic for the NRAO long-term technology program, and their successful development could have a huge impact on the performance of ALMA and other future radio telescopes. In this study, we describe our progress in developing both microwave (postdownconversion, or IF) and millimeter-wave (pre-downconversion, or RF) paramps during our on-going study. We designed and fabricated several versions of our IF paramps with improvements in gain, bandwidth, noise, dynamic range, gain ripple, pump power level, and chip footprint. We tested these in our JPL and NRAO/UVA shared testbeds and demonstrated that they can operate at 4 Kelvin while maintaining high gain ($\sim$15 dB) and wide bandwidth (6 GHz), although noise has not been tested at 4 K yet. When operated at $\leq$1 K, we consistently measured noise within a factor of two of the fundamental quantum limit for our IF paramps. At higher frequencies, we designed and fabricated several RF paramps with a simulated gain of $>$15 dB over the 65-150 GHz band, and made significant improvements in the fabrication methods. These chips have been mounted and are ready for testing in our W-band testbeds. In cycle 5, significant work was placed in building entirely new laboratory infrastructure at NRAO/UVA for testing both IF and RF paramps in a new testbed that can continuously operate the paramps at temperatures between 10 mK and 5 K. The results from our combined efforts at NRAO/UVA and Caltech/JPL and our new testbed infrastructure have put our team in an excellent position to continue this promising work, which is clearly synergistic with ALMAs roadmap.

The enhanced imaging capabilities that would be enabled by our proposed RF TKIP amplifiers would benefit a wide range of ALMA observations. For example, the Band-3 improved receiver noise performance from a front-end RF TKIP amplifier would increase the array efficiency (speed) by a factor of $\sim$4 enabling the detection of weaker spectral lines and continuum sources and mapping larger fields. The increased sensitivity from the RF front-end relaxes the

requirements on the IF amplifier and should allow the instantaneous bandwidth to be expanded from 16 GHz to ∼40 GHz. For continuum observations, this provides a factor of 2.5 increase in imaging efficiency (speed), which combined with the increased RF efficiency would result in a factor of 10 increase in observation efficiency (speed). For spectral observations such a wide bandwidth also enables the detection of various spectral lines simultaneously, removing the need of multiple observations at different LO frequencies to cover the whole band.

1. Science Case

1.1. Introduction

The noise temperature (TR) of radiometric receivers is the key parameter that impacts the overall performance of the system. Fig. 1 shows the single-sideband (SSB) noise temperatures of the current ALMA receivers as a function of frequency [1]. From this figure it is clear that there is still significant room for improvement in receiver noise performance before the theoretical limit of TR = hf/k for phase-coherent receivers is reached, a limit which is set by the quantum- mechanical uncertainty principle [2]. Superconductor- Insulator-Superconductor (SIS) mixers on ALMA followed by HFET intermediate-frequency (IF) amplifiers have reached their practical performance limits, except for bands 8, 9, 10 where materials such as NbTiN with larger gap energies could potentially be used to reach performance levels closer to the 4 hν/k trend line set by the lower- frequency bands. Although SIS mixers are nearly quantum limited, the inevitable conversion loss associated with downconversion from the input radio frequency (RF) to the IF implies that the IF amplifiers must have very low noise levels to not further reduce the signal integrity. The difficulty of achieving this low IF noise level over a wide IF frequency range is one of the fundamental factors limiting the instantaneous bandwidth of SIS receivers to ∼10 GHz [3]. Another key factor is the RC time constant of the SIS device, which is typically 10x or more slower at the IF as compared to the RF, and imposes a fundamental bandwidth limit as expressed by the Bode-Fano bound. A quantum-limited wide- band front-end TKIP amplifier receiver would circumvent this problem and would allow for both quantum-limited noise and wide instantaneous bandwidth.

In our currently on-going ALMA study from Cycle 5 (FY18-20), our team is investigating a breakthrough technology called the Traveling-Wave Kinetic Inductance Parametric (TKIP) amplifier [4]. These amplifiers are a new type of cryogenic power amplifier applicable in the microwave to THz range (0.001 to 1 THz) that exhibit ultra-low noise reaching the fundamental quantum limit, along with very wide bandwidth. The ALMA 2030 roadmap [6] recommends that "Long-term sustained research in better devices or new technologies (such as TKIP amplifiers) has the potential to yield significant breakthroughs that are equivalent to doubling or tripling the collecting area of the array with its present instrumentation." If suitably designed TKIPs could be used as front-end amplifiers for ALMA receivers [5] they could reduce the receiver noise temperature in every ALMA band, which would increase scientific productivity and would benefit science across all ALMA bands. Therefore, because of the potential game changing improvements that might be achieved it is important to further study these amplifiers with a long-term view of what will be

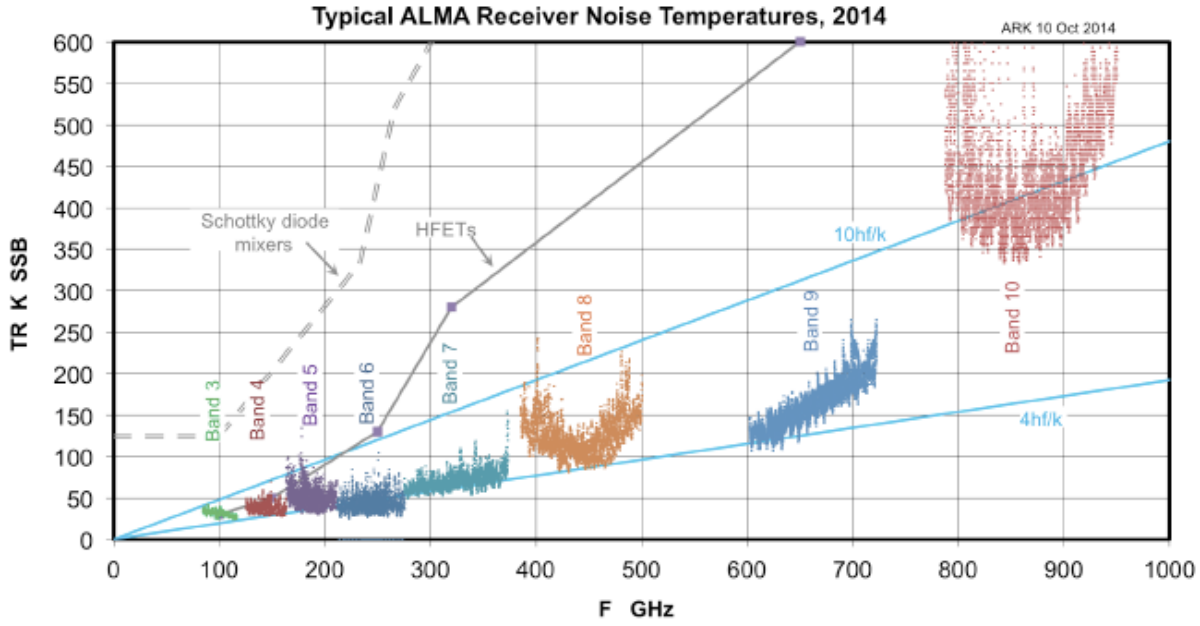

Fig. 1.— Single-sideband receiver noise temperature for typical ALMA SIS receivers. Bands 3-8 have sideband-separating mixers and bands 9 and 10 have double-sideband mixers. The noise temperatures shown for the DSB receivers are twice the DSB noise temperatures. Figure from [1].

possible in 5 to 10 years.

1.2. Increased Observation Efficiency with New Advanced Amplifiers

The enhanced imaging capabilities that would be enabled by our proposed RF TKIP amplifiers are impressive and would benefit a wide range of ALMA observations. For example, the Band 3 improved noise performance from a front-end RF TKIP amplifier on the receiver would be a factor of ∼5, which including the loss of atmosphere translates to a doubling of system sensitivity and a factor of ∼4 increase in array efficiency/speed (Fig. 2) enabling the detection of weaker spectral lines and weaker continuum sources for a given integration time. Provided the antenna response pattern is well measured, for a given sensitivity this leads directly to the ability to map larger fields due to the reduced integration time. Moreover, it allows for the use of weaker calibrators that are nearer to the source, improving not only image fidelity but also reducing the slew-time associated with calibrator observations.

The improvements resulting from an increase in receiver instantaneous bandwidth are also substantial. The large gain provided by the RF TKIP front-end substantially relaxes the requirements on IF noise and allows for tradeoff of noise with IF bandwidth. We expect this to easily allow an increase in the instantaneous IF bandwidth from 16 GHz (4 GHz per sideband per polarization) to ∼40 GHz (10 GHz per sideband

per polarization) and beyond, using commercially available LNA technology. This has a powerful impact on both continuum and spectral line observations. For continuum observations, this provides a factor of 2.5 increase in imaging efficiency, which combined with the increased RF efficiency would result in a factor of $\sim$10 in observation efficiency. For spectral observations such a wide bandwidth also enables the detection of various spectral lines simultaneously, removing the need for multiple observations at different LO frequencies to cover the whole band. This is also ideal for obtaining spectral index information on sources in much shorter integration times than is currently possible. In addition, as quoted from the ALMA 2030 roadmap document, "Bandwidth expansions will, simultaneously, enormously increase the legacy value of the archive while increasing the likelihood of serendipitous discoveries" [6].

1.3. Enhanced Science Studies

Studies of regions undergoing star and planet formation, molecular gas surveys, afterglows of Gamma-Ray Bursts (GRB), and objects in the high-redshift Universe are but a few of the current ALMA capabilities, which will be vastly improved by amplifiers from this proposed study. The increased continuum bandwidth will also allow for studies of clusters of galaxies, thought to be tracers of dark energy in the universe. Rather than describe the breadth of science that can be carried out with the new capabilities, we highlight one key program enabled by these amplifiers, as well as a few on- going programs that will benefit from these upgrades.

1.3.1. Clusters of Galaxies

The Sunyaev-Zeldovich (SZ) effect is a subtle distortion of the cosmic microwave background (CMB) spectrum caused by the scattering of CMB photons as they pass through the hot intracluster medium (ICM) of massive galaxy clusters. The brightness of this spectral distortion signal is independent of the redshift of the cluster. The SZ effect signal is proportional to the integrated pressure of the ICM plasma, which makes it an excellent proxy for cluster mass. These properties combine to make SZ surveys a unique tool for constraining cosmology, and large survey programs are now underway [7-9]. The SZ effect provides an important new window into the astrophysical processes that shape galaxy clusters, the most massive gravitationally bound objects in the universe. Recent observations of clusters of galaxies have shown a large fraction to have an irregular morphology due to merger events and feedback within the clusters. These are evidenced by the presence of shock fronts and cold fronts, as well as structure in these objects. With ALMAs high resolution and sensitivity, it is an ideal instrument for studying the cores of these objects and comparing these to high-resolution X-ray images.

One limitation of the current ALMA system in studying clusters of galaxies is that a large amount of the SZ signal comes from the outer regions of clusters. Being sensitive primarily to the core of the cluster, cluster observations with ALMA would require large integration times. With the increased bandwidth in continuum mode resulting from the proposed study, such cluster observations would be obtainable in a

matter of hours, expanding on the current capabilities of the array.

1.3.2. Star Formation in the Milky Way (through spectral and continuum observations)

Star formation in the Milky Way takes place in molecular clouds that can contain upwards of 10^6 $M_\odot$ of gas and dust [10]. At any instant, only a few percent of the cloud mass has achieved sufficiently high density to form stars [11]. The dominant mass and volume of clouds are in a low-density molecular state that is devoid of active star formation. The transition from a low-density state to a star-forming state is the first and biggest step on the path to stars. Understanding how this happens and why such a small fraction of the cloud mass is contained in dense gas is key to determining the dominant physical processes that control the star formation rate in molecular clouds in our Galaxy.

In practice, no single molecule can probe the cloud structure over all scales. Each molecular transition probes different volume densities and temperatures, and time- dependent chemistry favors the production of different molecules at distinct times. With 40 GHz of instantaneous bandwidth, ALMA would have the tremendous flexibility to observe multiple molecular transitions simultaneously and probe these different regions. With the increased speed in mosaic observations enabled by this study, ALMA mosaics will provide tens of thousands of independent resolution elements in which to measure the cloud structure and kinematics.

In addition to spectral observations of molecules, this development would improve the ability of ALMA to perform continuum surveys of protostellar disks. These dusty disks are expected to evolve as dust grains settle to coalesce into larger solid bodies, potentially forming planets. This evolution can be traced by determining the dust SED of a coherent sample of protostellar disks, and studies are currently underway aimed at determining the dust temperature, emissivity properties, and optical depth. These studies use multiple ALMA bands, which would be done with greater efficiency with the results from this proposal.

1.3.3. Survey of Molecular Gas and Dust in Submillimeter Galaxies

Submillimeter galaxies trace a large fraction of the star formation activity at the epoch of galaxy evolution ($1 < z <¡ 3$). These SMGs have been detected with single-dish telescopes with coarse resolution, and counterpart identification requires deep radio observations followed by deep optical and near-infrared spectroscopy. ALMA can currently locate SMGs precisely and obtain a redshift using sequential observations to cover an entire ALMA band to detected one or more redshifted CO lines. Covering the whole ALMA band 3 requires setting the LO to 5 different frequencies and integrating at each of those. The proposed study would speed up this process not only by increasing the overall sensitivity of the band, but also by covering the full band 3 simultaneously (with no need to tune the LO).

1.3.4. Molecular Absorption lines at high redshifts

One means of determining the composition of the interstellar medium of a foreground galaxy is by observing the gas in absorption against a bright background continuum source. This method is very powerful because the detectability of the intervening gas depends only on the brightness of the background source. A recent example of such a study [12] reports on detections of [C II] 158-μm line and dust-continuum emission from two galaxies associated with two such absorbers at a redshift of z $\sim$ 4. The results of this study indicate that the hosts of these high-metallicity absorbers have physical properties similar to massive star-forming galaxies and are embedded in enriched neutral hydrogen gas reservoirs that extend well beyond the star-forming interstellar medium of these galaxies. In its current state, ALMA will allow for an unbiased survey for absorption lines in selected distant galaxies such as these, but will do so with relative inefficiency. The results of the proposed study could greatly increase the efficiency with which these studies are performed, resulting in more detailed determination of the molecular gas properties of these absorption line systems, or a larger sample on which a statistical analysis could be performed.

2. Study Scope

2.1. Bandwidth and Sensitivity Benefits of TKIP Amplifiers for ALMA

Implementing a TKIP amplifier at the RF front-end of a receiver would greatly improve the state-of-the-art of heterodyne receiver systems by providing a low-noise gain element directly at millimeter/submillimeter wavelengths. We consider here the ALMA band-3 case as an example. The current Band 3 receivers have noise temperatures of $\sim$38K over the 84-116 GHz band (Fig. 2 (Left) [14]). The quantum limit to noise contribution from the amplification process ($\frac{1}{2}$ photon) in this frequency range is $\sim$ 2.5 K, and there is an additional $\sim$ 2.5 K contribution from the quantum vacuum fluctuations and $\sim$2 K of noise contribution from lossy optical components [14]. If we make the best-case assumption that the amplifier is quantum-noise limited, then **a factor of $\sim$5 improvement in receiver noise temperature would be realized using an RF TKIP amplifier operating at the quantum limit. This translates to a doubling of system sensitivity and a factor of four increase in observation efficiency/speed of the array.** Figure 2 (Left) shows the current performance of Band 3, and Fig. 2 (Right) shows the expected performance improvement from an RF TKIP amplifier. Note that this does not consider possible further improvement from replacing the IF amplifiers with wider bandwidth amplifiers.

Although the SIS mixers in ALMA are quantum-limited, during the heterodyne frequency down- conversion process in the mixer they introduce about 6 dB of RF-to-IF conversion loss. Therefore, the input to the IF amplifier becomes the point of lowest signal level in the entire receiver system, so the IF amplifier must have very low noise. The difficulty of achieving a low noise level over a wide IF frequency range is currently a limitation to instantaneous bandwidth [3], and has limited SIS receiver bandwidths to 10 GHz. Current state-of-the-art technologies, including the best InP HEMT amplifiers, have achieved their practical limits in noise temperature [13]. Therefore, the use of the new TKIP RF amplifier technology to

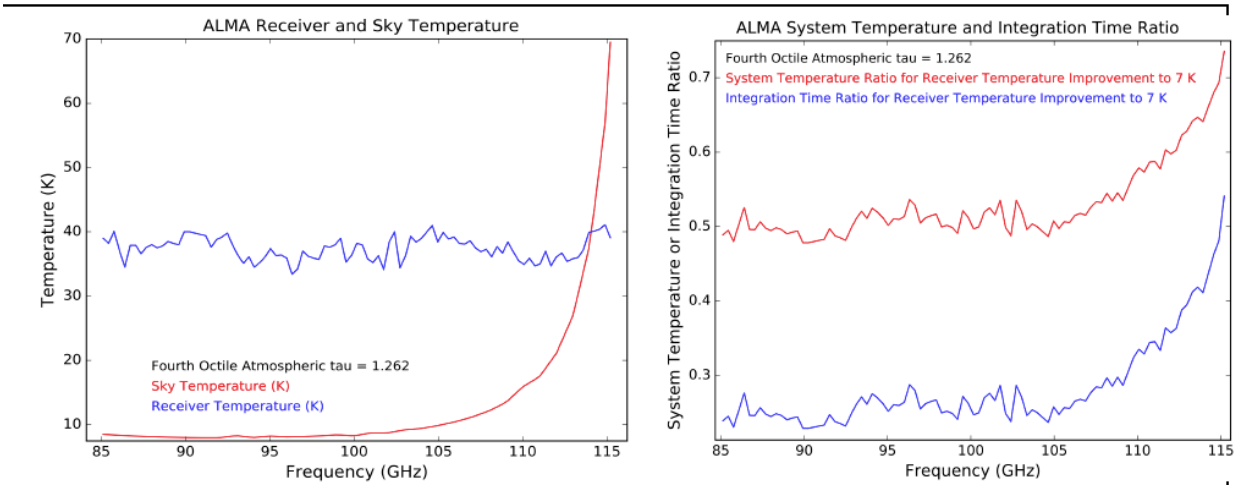

Fig. 2.— Sensitivity calculation for ALMA band 3 using data and formalism described in [14, 15]. (Left) Actual Band 3 receiver noise temperature measured on the current ALMA array (extracted from the thousands made during 2016) with sky noise temperature assuming fourth-quartile weather conditions (typical for Band 3). (Right) Total system noise temperature and integration time improvement ratios assuming receiver noise improves from 38 K to 7 K with a quantum-limited TKIP amplifier. System noise improves by a factor of ~ 2 and integration time reduces by a factor of ~ 4 and. If the current 4-GHz IF amplifiers in ALMA are replaced by 10-GHz amplifiers (enabled by relaxed IF noise requirements), the integration time reduces by another factor of 2.5 to a total of 10.

provide gain before the mixer would greatly relieve the requirements on the following components. Not only would it be easier to approach the quantum limit with such a receiver, **but the IF bandwidth could then be easily widened from 16 GHz (4 GHz per sideband per polarization) to 40 GHz, increasing the speed for line surveys by an additional factor of 2.5 and greatly improving the sensitivity for continuum observations.**

2.2. Traveling-Wave Kinetic Inductance Parametric (TKIP) Amplifiers

Parametric amplification has long been known as a technique for achieving the ultimate in low noise performance. A purely reactive (lossless) nonlinearity can be utilized to amplify a weak signal in the presence of a strong pump tone without the addition of noise that is associated with dissipative components. Theoretically, such an amplifier can reach the fundamental limits set by quantum mechanics of adding $\frac{1}{2}$ photon of noise referred to the input signal in addition to the $\frac{1}{2}$ photon of vacuum fluctuations, for a total of one photon of noise [2]. Parametric amplifiers using various nonlinear components such as varactor diodes were common in the past and are still in use in some satellite communication stations. However, none were without dissipative loss and so reaching the quantum limit was not possible. In the optical domain, parametric amplifiers (paramps) based on the Kerr effect have achieved near quantum-limited performance with

high gain at optical wavelengths [16] due to the very low loss nature of optical fibers.

In the microwave domain, two types of low-noise cryogenic amplifiers are currently in use. The conventional type uses transistors made of semiconducting materials (silicon-germanium or indium- phosphide) and is typically cooled to 4 Kelvin. Their best achievable noise level is about five times the quantum limit, limited by noise in the transistor and loss from passive components [3]. The second type uses superconducting Josephson tunnel junctions (Josephson Parametric Amplifier or JPA) to produce parametric nonlinearity [17, 18, 19]. These, however, operate at $<$100mK temperatures and although they reach the quantum noise limit they typically have a narrow bandwidth (few MHz) or small dynamic range ($<$-100 dBm), which has excluded their application for radio astronomy.

In 2012 our collaborators at Caltech and JPL (Day et al.) achieved a breakthrough in paramp technology [4]. They demonstrated a new type of paramp with near quantum-limited noise in the 9-14 GHz range and high dynamic range ($\sim$-50 dBm). Their amplifier, which is named a *Traveling-Wave Kinetic Inductance Parametric (TKIP) amplifier*, was made from a 0.8-meter-long spiral of 35-nm-thick NbTiN coplanar waveguide transmission line on silicon with a 1-micron-wide center conductor and a 1-micron gap to the neighboring ground plane. Due to the much higher critical current of a superconducting film vs. a Josephson junction, this type of amplifier exhibits a saturation power that is *5-6 orders of magnitude* higher than JPAs, making it more suitable for ground-based astronomy.

The TKIP amplifier exploits the reactive nonlinearity of a superconducting NbTiN transmission line to produce gain. The nonlinearity comes from the current-dependent kinetic inductance (the kinetic inductance results from the storage of kinetic energy associated with the motion of superconducting electron pairs carrying the non-dissipative supercurrent) that can have a dominant effect on the line characteristics. The nonlinearity has the effect of making the effective phase velocity of the transmission medium dependent on the intensity of a wave propagating along it; that is, the line is a Kerr medium, analogous to nonlinear optical fibers. This nonlinearity can be used to produce parametric gain in a travelling-wave geometry, which is intrinsically broadband. A strong pump tone at ω_p is injected into one end of the device along with the weak signal at s. The nonlinearity of the medium mediates the transfer of power from the pump to the signal through frequency mixing and produces gain. As a side-product, an idler signal is also produced at i. Depending on the device design the energy conservation law imposes a relation between these signals that is $\omega_s + \omega_i = 2\omega_p$ (in the case of 4-wave mixing) or $\omega_s + \omega_i = \omega_p$ (3-wave mixing) [20]. In the case of 3-wave mixing, a DC bias is also applied to the device in addition to the AC pump tone, which allows for a reduced AC tone power. In this case, the pump frequency falls outside of the gain profile, which makes it convenient to filter the pump tone at the output of the paramp using a low-pass filter. TKIPs also require momentum conservation, i.e., phase matching, for the pump, signal, and any idlers that are generated to achieve wideband gain. Momentum conservation can be attained by dispersion engineering of the line: periodic loadings are used to create a narrow stop band (a band gap), and due to the Kramers-Kronig relations, there is an associated frequency-dependent phase velocity. If the pump frequency is tuned close to this band gap, the dispersion-induced phase shift will add to its self- phase modulation, allowing it to match its cross-phase modulation to other signals on the line [21], and parametric amplification can occur. Because the signal and idler frequencies lie on relatively linear portions of the dispersion curve, far from the

narrow stop band, a wide signal bandwidth can be obtained.

In addition to allowing more bandwidth and saturation power, the TKIP amplifier is directional so that amplification only occurs for signals propagating in the same direction as the pump.

The concept of the TKIP can be applied to frequencies up to around the gap frequency of NbTiN ($<$1.4 THz), beyond which photons break Cooper pairs and generate resistive loss. This has opened up the possibility to develop these amplifiers for ALMAs mm/submm font-ends as RF amplifiers. The lower frequency limit is determined only by the length of transmission line that can be fabricated, a limit that in practice is set by fabrication yield.

2.3. Results from our on-going TKIP Amplifier Study Proposal

In an on-going ALMA cycle 5 strategic study (FY18-20) that was titled "Quantum-Limited Very- Wide-band 4-Kelvin RF and IF Amplifiers for ALMA" we proposed to study both IF an RF (W-band) paramps. We made significant progress on several fronts relevant to this proposal, which we briefly summarize below. These results as well as our efforts in building a complete IF and RF (W-band) cryogenic testbed for paramps at NRAO/UVA and JPL have put our team in an excellent position to continue this promising work.

2.3.1. Quantum-limited wideband IF TKIP amplifiers

In our on-going study, we designed and fabricated several different IF paramps based on either a coplanar-wave (CPW) or a microstrip-line geometry in the $\sim$ 4 to 14 GHz range. A central focus of that study was the testing of these amplifiers at elevated temperatures close to 4 Kelvin to evaluate compatibility with the ALMA cryocoolers. We tested these in our JPL and NRAO/UVA testbeds and confirmed that they maintain their lower-temperature gain of $>$15 dB over a $>$6 GHz bandwidth even when at 4 Kelvin. We also consistently measured noise within this bandwidth within a factor of two of the vacuum fluctuation level for these devices when operated at $<$1 Kelvin.

The first TKIP design from the 2012 article [4] used a regular CPW geometry that was very long ($\sim$ 0.8 meter) to obtain sufficient gain. However, because of the high kinetic inductance of NbTiN the impedance of the line was $\sim$ 200-300 Ohm. To impedance match this to the outside 50 Ohm circuitry, long tapered transformers were used on both sides on the chip; however, these did not result in sufficiently reduced gain ripples. Furthermore, the long length of the line meant that fabrication defects were more likely to exists and cause a break or non-uniformity in the width of the line, which could result in reduced gain and dynamic range. Since then we developed two new designs that overcome these problems.

In one new design, we use a comb of interdigitated capacitors (IDCs) in the CPW line to increase the capacitance per unit length of the line, which has the effect of reducing the characteristic impedance to 50 Ohm. Another important improvement is the reduced phase velocity caused by the additional capacitance. This has the effect of increasing the electrical length of the line thereby allowing a much shorter physical

length (2.5 cm vs 80 cm) to achieve a given gain. The fabrication yield is also higher for these smaller devices as compared to the 0.8-meter-long devices, since defects are less likely to cause a break in the main line and a broken IDC finger will not substantially impact the operation of the amplifier. We tested several iterations of this type of CPW paramp, which also included additional structures for gap engineering and phase matching. Figure 3 shows an example of a measured device of this type performed with 3-wave mixing, and exhibits a beautifully flat gain profile with significantly reduced ripples. The gain was measured when the device was operated at 4 Kevin in a liquid helium dipping probe setup. We also consistently measured added amplifier noise that is within a factor of two of the quantum limit of a $\frac{1}{2}$ photon, when the device was operated at 40 mK in a dilution refrigerator. We have not measured noise at higher device temperatures yet but plan to do so in our on-going cycle-5 study.

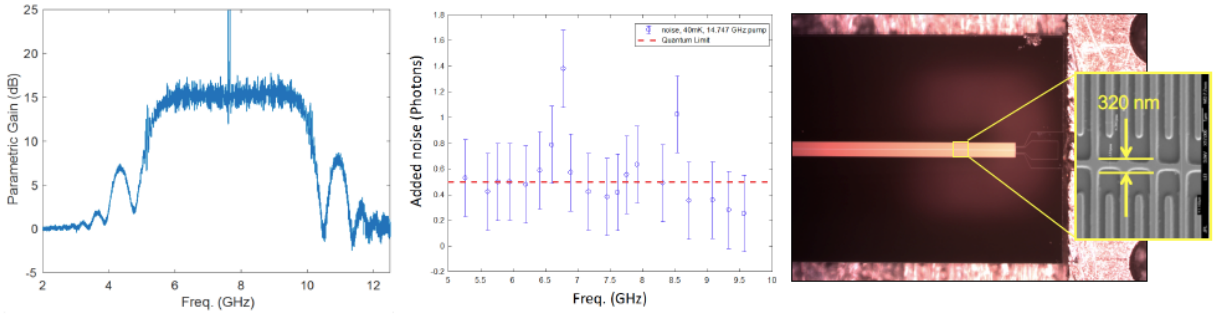

Fig. 3.— (Left) Gain of a CPW-based paramp measured at JPL with a pump tone at 15.25 GHz and pump power in the range of 0.2 - 2 microWatt. The spike is a data artifact and not real. (Middle) Noise contribution of the same paramp (in addition to the $\frac{1}{2}$ photon vacuum noise), measured using the y-factor method, is at the quantum level. (Right) Photograph of device with a zoom-in of a section of the traveling-wave interdigitated CPW line. The amplifer is a 2.5-cm-long CPW, with a line and gap with of 320 nm and is made of 35 nm of NbTiN on Si.

In a more recent design, we used a two-metal-layer inverted microstrip geometry instead of a single-layer CPW. The inverted structure has the advantage that it protects the narrow 250-nm microstrip line under a layer of dielectric and metal ground plane, and increases the fabrication yield and device uniformity. We used a 300-nm-thick layer of deposited amorphous silicon (a-Si) for the dielectric layer, and 35-nm-thick NbTiN top and ground-plane microstrip layers on a silicon substrate. A key innovation here is the use of very low loss a-Si [22] that was developed at JPL that exhibits loss tangent of order 1x10^{-5} or lower, which minimizes the impact of two-level-system (TLS) dielectric losses that commonly limit the performance of high-Q superconducting circuits, and mitigates any potential added noise that can arise from loss. Fine-tuning of the thickness of this layer allows for fine adjustments of the impedance match, and we have successfully explored this ability to some extent using post-measurement simulations of devices to iterate the thickness of this layer. We also used an interdigitated capacitor geometry similar to the CPW design to simultaneously reduce the phase velocity of the line to $\sim$ 0.007c (and 2.5 cm line length) and significantly bring down the impedance closer to 50 Ohm. The measured gain and noise performance of this amplifier

are shown in Fig. 4. The performance is similar to the CPW device in both gain and noise. The errors in the noise measurement data are due to temperature drifts in the noise measurement setup over the relatively long measurement time that was needed, and we are working to improve this. More recent versions of this type of device show reduced levels of gain ripple, which indicates that controlling the impedance is key to reducing ripple.

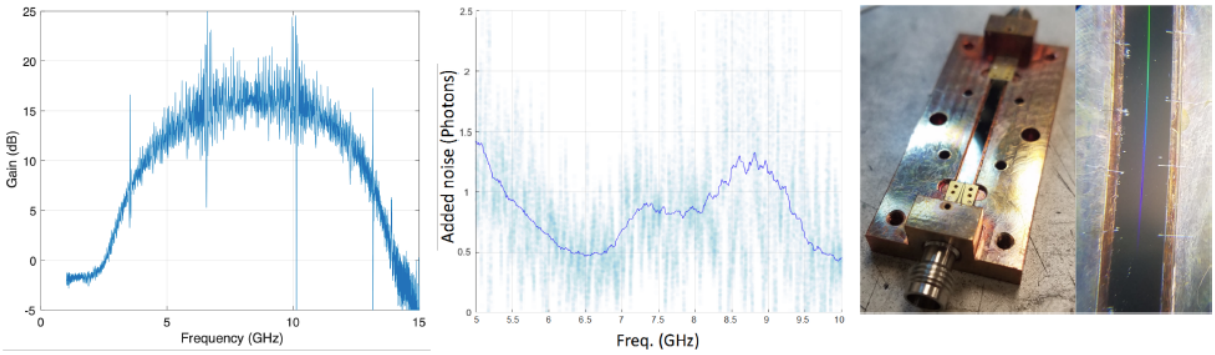

Fig. 4.— (Left) Gain of a microstrip-based paramp measured at 4 Kelvin at JPL with a pump tone at 16.7 GHz and pump power of $\sim$ 2 microWatt (-27 dBm) and DC bias of 0.5 mA. (Middle) Noise contribution of the same paramp operated at 40 mK, measured using the y-factor method, is within a factor of two of the quantum level. (Right) Photograph of packaged device with a zoom-in of a section of the traveling-wave interdigitated microstrip-line with the ground-plane wirebonded to the box. The amplifer is a 2.5-cm-long inverted microstrip, with a 35-nm-thick NbTiN line width of 250 nm and interdigitated finger lengths of 14 micron.

2.3.2. Effect of high-temperature (4-Kelvin) operation on IF paramp gain

We tested in our new NRAO/UVA cryogenic testbed one of our previously measured paramps at JPL, in order to explore the effect of higher temperature on the gain of paramps, as well as to crosscheck the reliability of our new testbed to perform such tests. One of the advantages of our NRAO/UVA testbed is that it allows for a continuous sweep of the device temperature from 10 mK to $\sim$ 5K while installed on the lowest base temperature stage of our dilution fridge in one cool down. Normally, this is not easily doable because of the 3He/4He mixture temperature and pressure constraints, but our newly installed system accommodates this. In Fig. 5 we can see that the gain of the device at 100 mK and 3.93K is very similar. The ripple magnitude is significantly reduced which indicates that loss mechanisms are dampening the internal reflections inside the paramp. From the ripple periodicity, we confirmed that the ripples are indeed from inside the paramp and not from other components in the testbed, so we believe that thermally-generated quasiparticles in NbTiN are responsible for the added loss. Therefore, to operate the paramp at $\sim$

4K with minimum loss (and hence added noise) the critical temperature (Tc) of the film should be increased. This materials fabrication challenge is an area that we propose to study in a future proposal.

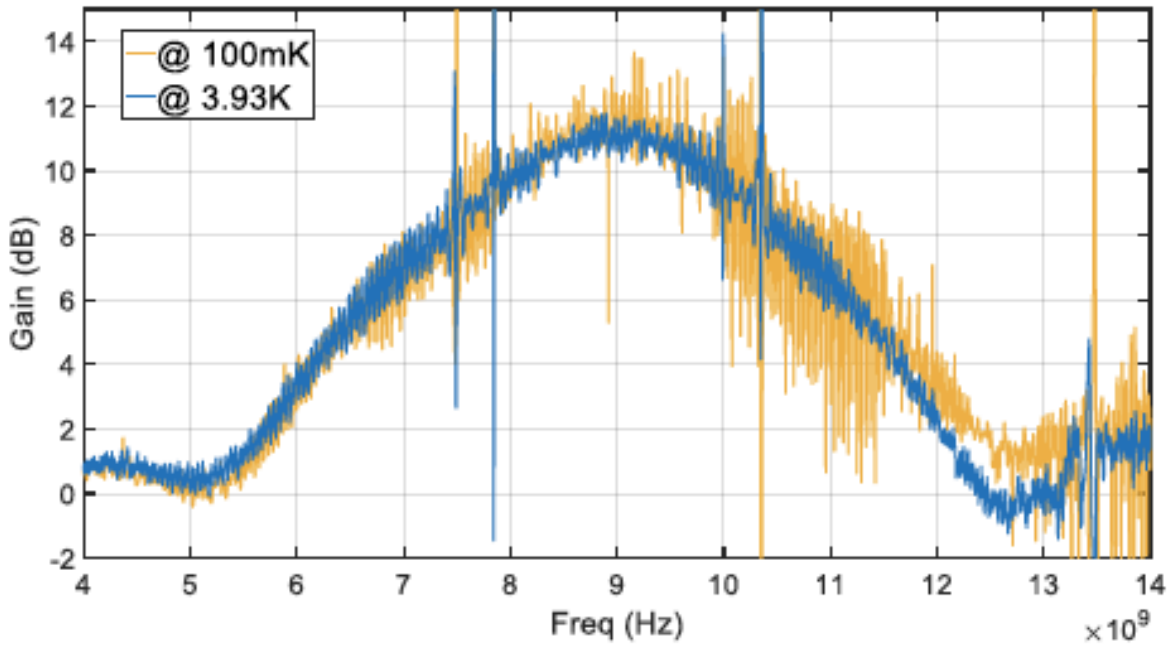

Fig. 5.— Comparison of paramp gain measured at 3.93 K and 100 mK for a microstrip-based device (tested at NRAO/UVA). The device was operated in 4-wave mixing mode with an 8-microWatt pump tone at 8.92 GHz. Ripples are significantly reduced at the expense of added quasiparticle losses at 3.93 K.

2.3.3. Ultra-wideband (65-150 GHz) RF TKIP amplifiers

We chose to focus our RF demonstration effort on a TKIP amplifier suitable for ALMA Band 3 (84-116 GHz). This particular band was chosen since it is at high enough frequency that a demonstration of near-quantum-limited wideband gain would be valuable toward establishing these amplifiers for millimeter- and submillimeter-wave receivers. In addition, the frequency is low enough that these devices could be tested with commercial network and spectrum analyzers in the W-band (75-110 GHz).

Based on successful results from our IF TKIP amplifiers, **we designed, simulated, and fabricated a new microstrip-based RF TKIP amplifier that covers the 65-150 GHz range with a >15 dB gain** (see Fig. 6). Impressively, this range fully covers ALMA bands 2 (65-90 GHz) and 3 (84-116 GHz), and part of band 4 (125-163 GHz) simultaneously. A simulation of gain for this paramp is shown in Fig. 6 (Right). The chip is made of a 1.9-cm-long and 2-micron-wide 35-nm-thick NbTiN microstripline meander on silicon with 300 nm of a-Si dielectric on top and a NbTiN groundplane (top side of the photograph). The silicon substrate is 25 microns thick and is produced through a silicon-on-insulator (SOI) wafer process. This device has been successfully fabricated and packaged in a split-block waveguide box (Fig. 6 (Left)), and is ready for testing. The signal and pump enter through a WR-10 waveguide, and transition from waveguide mode to microstrip mode using an on-chip probe antenna that was designed with HFSS to provide efficient coupling (see Fig. 7).

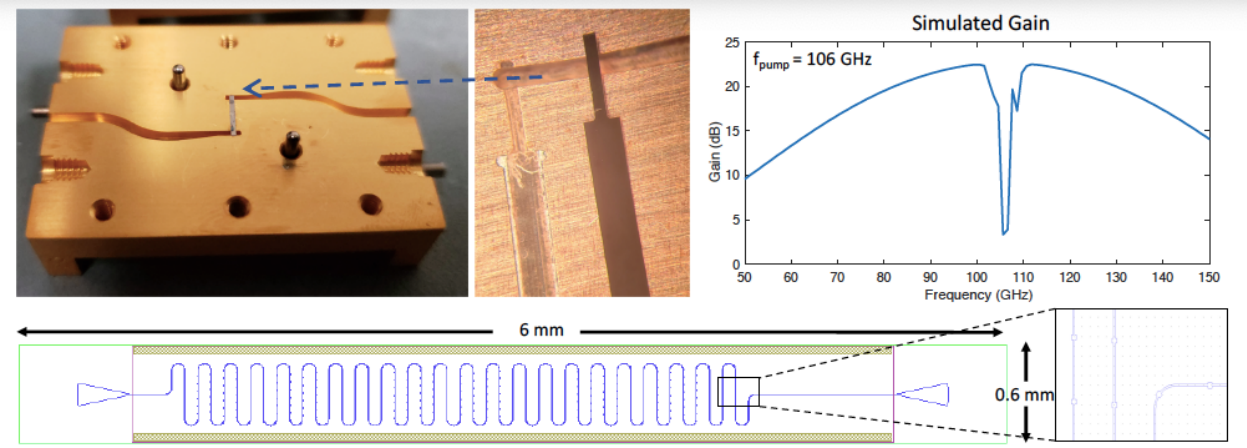

Fig. 6.— (Left) Packaged RF TKIP amplifier with a zoom-in of the waveguide-to-chip transition area. (Right) Simulated gain profile of this amplifier with a notch around the pump tone. (Bottom) Circuit layout as implemented on the fabrication mask. A zoom-in of a section of the microstrip-line with periodic structures for wideband phase matching and 3rd harmonic suppression.

2.3.4. Microwave/Millimeter-wave cryogenic testbed at NRAO/UVA

At NRAO/UVA we spent significant time on building the foundations of entirely new laboratory infrastructure that was needed for this project, including procuring and building a new cryogenic testbed that can continuously operate between 10mK and 5K. Although the funding needed for acquiring the cryostat and parts for this testbed was delayed by $\sim$ 1 year, we were able to equip the cryostat with custom cryogenic components (superconducting coaxes, filters, LNAs, etc.) and room-temperature readout electronics, and successfully tested an IF paramp in this system. We also designed, built, and tested custom WR-10 waveguide components needed for the high-frequency RF testbed, including a series of waveguide thermal isolators and waveguide vacuum feedthroughs. In our design, the thermal isolation of the cryostat stages, as well as isolation of the paramp from cryogenic blackbody thermal loads (needed for noise testing) is achieved using a series of custom WR-10 isolators that employ a small physical gap of $\sim$ 1 mil between two waveguides [23]. A periodic bandgap structure at the joint suppresses fields propagating between the two parallel conducting surfaces and improves overall transmission. Our measurements of these at NRAO/UVA indicate <-25 dB input reflection and <0.2 dB transmission loss, as shown in Fig. 8 (Left). We also designed and built vacuum feedthroughs that use a 15-micron-thick mica disk as a vacuum window between two WR-10 waveguides. These were measured to have $\sim$ 0.4 dB of transmission loss, about -20dB of input reflection (Fig. 8 (Right)), and a vacuum helium leak rate of $\sim$ 1e-7 mbar*L/s that meet our requirements.

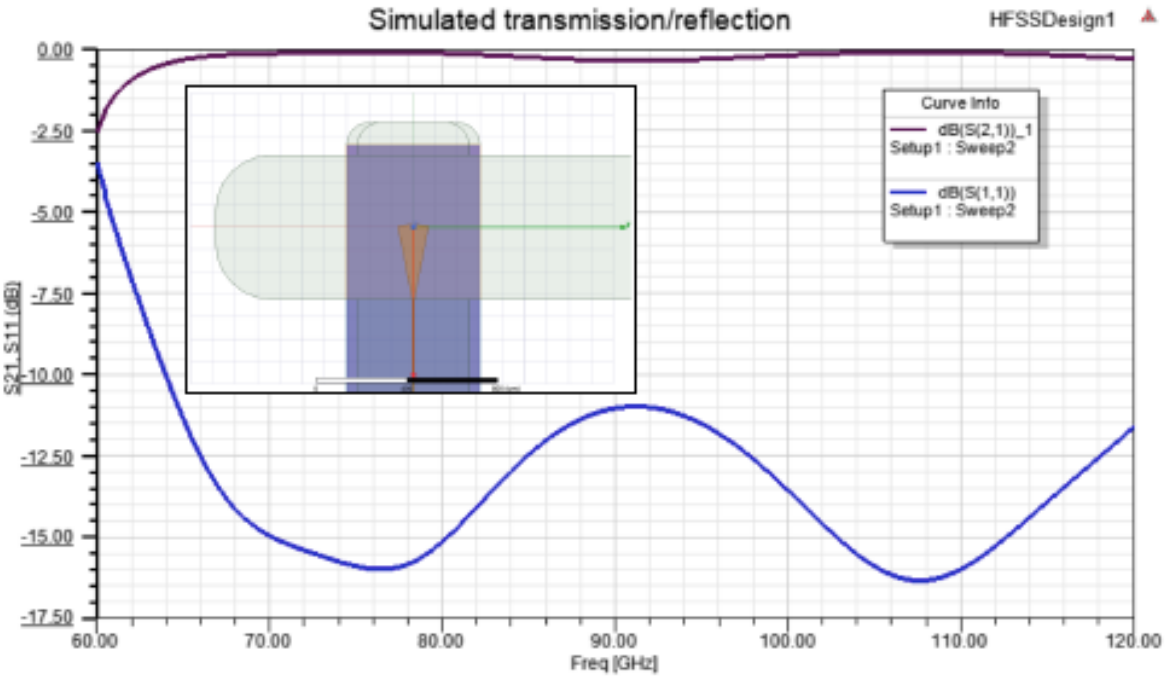

Fig. 7.— Simulated waveguide-to-microstrip probe antenna that is integrated on the TKIP amplifier chip, with near lossless transmission and <-10 dB reflection. Inset shows an HFSS model for the WR-10 waveguide cavity loaded with the on-chip probe section that is made from 35-nm-thick NbTiN on a 25-micron-thick silicon chip.

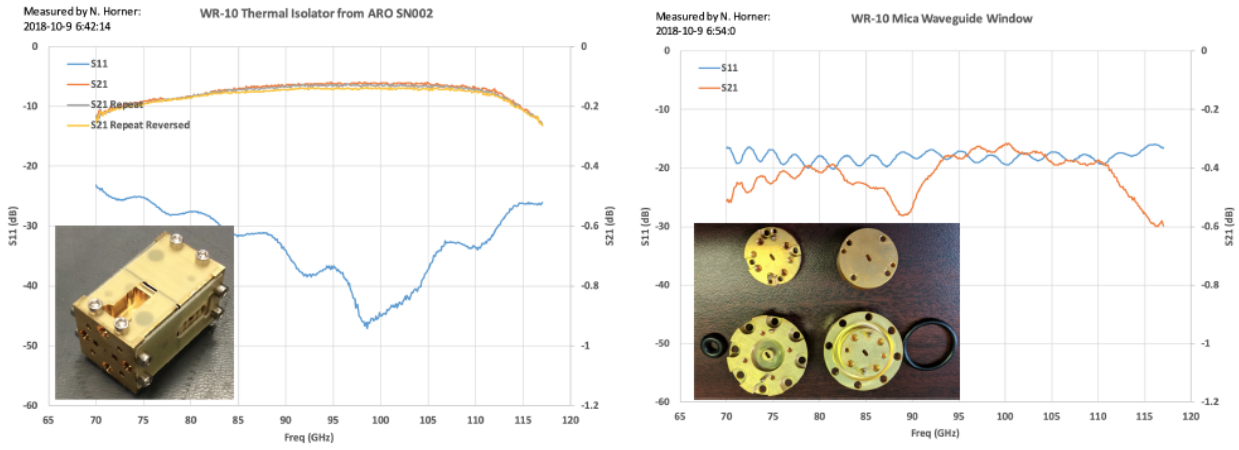

Fig. 8.— (Left) Measured S_21/S_11 for a gap-based WR-10 waveguide thermal isolator. (Right) Measured S_21/S_11 for a custom-made WR-10 vacuum feedthrough with a 15-micron-thick mica disk vacuum window.

References

1. A. R. Kerr, S.-K. Pan, W. G. Lyons, "The Genesis of SIS Mixers The Legacy of John Tucker in Radio Astronomy," 2015 IEEE International Microwave Symposium, invited paper, Special Tribute Session to Prof. John R. Tucker, (2015).

2. C. M. Caves, Physical Review D, vol. 26, pp. 1817, (1982).

3. M. Pospieszalski, A. Kerr, J. Mangum, On the Instantaneous SIS Receiver Bandwidth, ALMA Memo 601, (2016).

4. B. H. Eom, P. K. Day, H. G. LeDuc, and J. Zmuidzinas, A wideband, low-noise superconducting amplifier with high dynamic range, Nature Physics, Vol. 8, p. 623 (2012).

5. D. Woody et al., Final Report on Development of ultra-wideband quantum limited amplifiers for millimeter and submillimeter receiver frontends, (2013).

6. https://go.nrao.edu/Roadmap_for_ALMA

7. J.C. Carlstrom, et al., The 10 Meter South Pole Telescope, Publications of the Astronomical Society of the Pacific, Vol. 123, pp. 568-581, (2011).

8. J. Fowler, et al., Optical design of the Atacama Cosmology Telescope and the Millimeter Bolometric Array Camera, Appl. Optics, Vol. 46, pp. 3444-3454, (2007).

9. Planck Collaboration, et al., Planck early results. VIII. The all-sky early Sunyaev-Zeldovich cluster sample, Astronomy and Astrophysics, Vol. 536, (2011).

10. N. Scoville, et al., Molecular clouds and cloud cores in the inner Galaxy, Astrophysical Journal Supplement, Vol. 63, p.821-915, (1987).

11. D. Johnstone et al., An Extinction Threshold for Protostellar Cores in Ophiuchus, Astrophysical Journal, Vol. 611, pp. 45-48, (2004).

12. M. Neeleman et al., [CII] 158-m emission from the host galaxies of damped Lyman-alpha systems, Science, Vol. 355, p. 1285, (2017).

13. J. Schleeh, J. Mateos, I. niguez-de-la-Torre, N. Wadefalk, P. A. Nilsson, J. Grahn, A. J. Minnich, Phonon black-body radiation limit for heat dissipation in electronics, Nature Materials, Vol. 14, pp.187-192, (2015).

14. A. R. Kerr et al., Development of the ALMA Band-3 and Band-6 Sideband-Separating SIS Mixers, IEEE Trans. on Microwave Theory and Tech., Vol. 4, No. 2, (2014).

15. J. Mangum, ALMA Sensitivity Metric for Science Sustainability Project, ALMA Memo 602, (2017).

16. J. Hansryd, P. A. Andrekson, Fiber-Based Optical Parametric Amplifiers and Their Applications,

IEEE Journal of Selected Optics In Quantum Mechanics, Vol. 8, No. 3 (2002).

17. H. Zimmer, Parametric amplification of microwaves in superconducting Josephson tunnel junctions, Appl. Phys. Lett., Vol. 10, pp. 193195 (1967).

18. K. OBrien, C. Macklin, I. Siddiqi, and X. Zhang, Resonant Phase Matching of Josephson Junction Traveling Wave Parametric Amplifiers, Physical Review Letters, vol. 113, pp. 157001, (2014).

19. C. Macklin, K. OBrien, D. Hover, M.E. Schwartz, V. Bolkhovsky, X. Zhang, W.D. Oliver, and I. Siddiqi, A near-quantum-limited Josephson traveling-wave parametric amplifier, Science, vol. 350, pp. 307-310, (2013).

20. M.R. Vissers et al., Low-noise kinetic inductance traveling-wave amplifier using three-wave mixing, Applied physics letters, 108, (2016).

21. G. P. Agrawal, Applications of nonlinear fiber optics (ed Agrawal, G. P.) (2001).

22. A.D. O'Connell et al., Microwave dielectric loss at single photon energies and millikelvin temperatures, Applied Physics Letters 92, 112903, (2008).

23. J.L. Hesler, A.R. Kerr, N. Horner, A Broadband Waveguide Thermal Isolator, Proc. 14th International Symposium on Space Terahertz Technology, p.148-154, (2003).